Remote Sensing of Wildland Fire-induced Risk
Assessment Framework

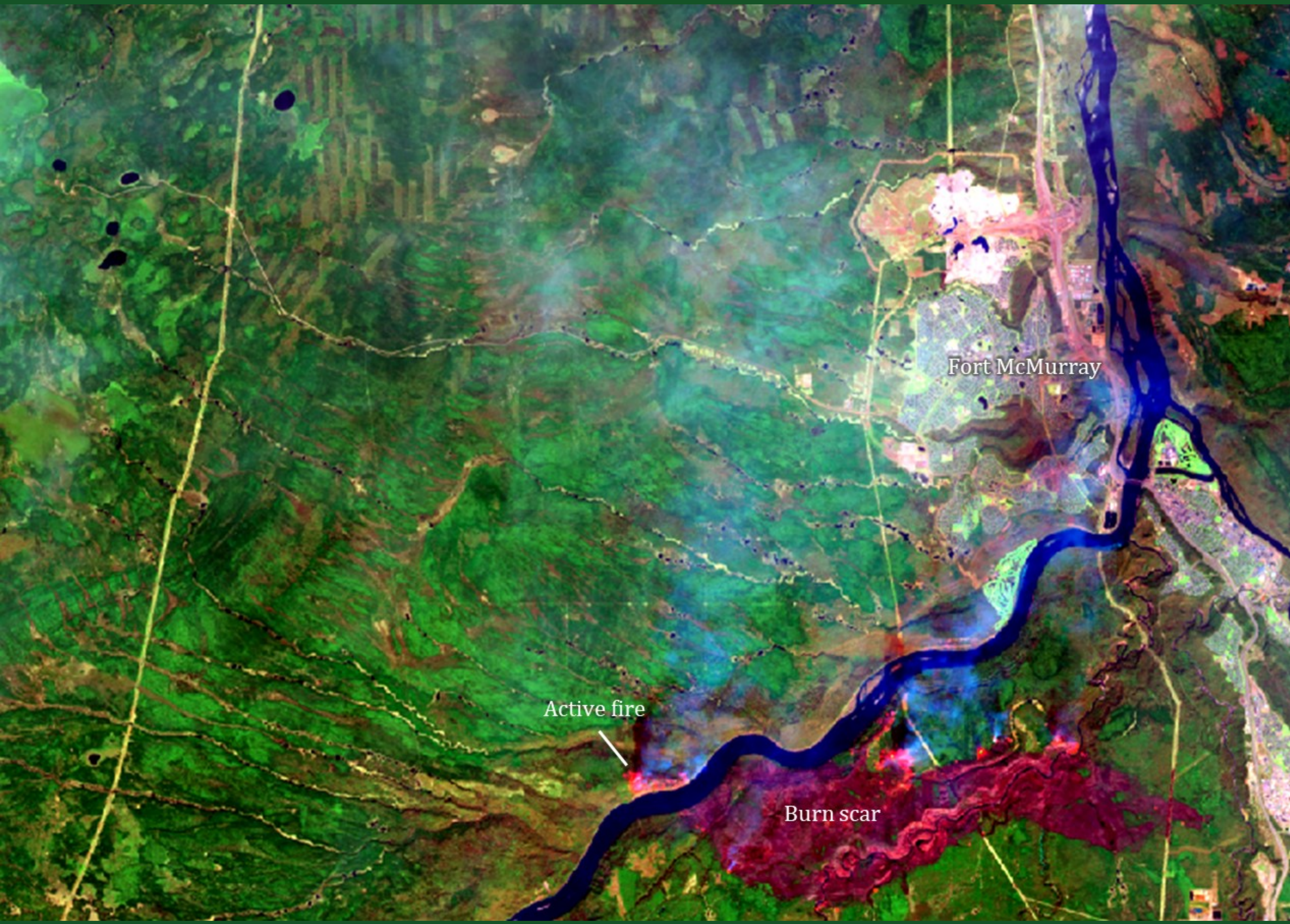

Quazi K. Hassan, M. Razu Ahmed, Khan R. Rahaman

December 2017

University of the Fraser Valley
Centre for Public Safety & Criminal Justice Research

Schulich School of Engineering
University of Calgary

EARTH OBSERVATION FOR ENVIRONMENT LABORATORY

The Earth Observation for Environment Laboratory is part of the Department of Geomatics Engineering and Centre for Environmental Engineering Research and Education in the Schulich School of Engineering at the University of Calgary. The Laboratory is led by Professor Dr. Quazi K. Hassan. The mandate of this lab is to lead cutting edge research in addressing environmental issues by integrating remote sensing, GIS, and modelling techniques.

Authors: Quazi K. Hassan, M. Razu Ahmed, Khan R. Rahaman.

Suggested citation: Hassan, Q.K.; Ahmed, M.R.; and Rahaman, K.R. (2017). Wildland Fire-induced Risk Modelling Framework for the Greater Athabasca Oil Sand Region, A Report for the National Fire Information Database (NFID) Project, Vancouver, BC. December, 2017.

For any questions regarding this report, please contact:

Dr. Quazi K. Hassan
Earth Observation and Environment Laboratory
Department of Geomatics Engineering, and Centre for Environmental Engineering Research and Education
Schulich School of Engineering
University of Calgary
2500 University Drive NW, Calgary, AB T2N 1N4

Email: qhassan@ucalgary.ca
Phone: 403 – 210 – 9494

Cover image: Processed by authors using Landsat-8 OLI data acquired on 3 May 2016 available from the U.S. Geological Survey. The image is a false color composite of shortwave infrared, near infrared, and green spectral bands.

Table of Contents

Executive Summary

Wildland fire is one of the critical natural hazards that pose a significant threat to the communities located in the vicinity of forested/vegetated areas. In this report, our overall goal was to use very high spatial resolution (0.5-2.4m) satellite images to develop wildland fire-induced risk framework. We considered two extreme fire events, such as the 2016 HRF over Fort McMurray, and 2011 Lesser Slave Lake fire in Alberta. Thus, our activities included the: (i) estimation of the structural damages; and (ii) delineation of the wildland-urban interface (WUI) and its associated buffers at certain intervals, and their utilization in assessing potential risks. Our proposed method of remote sensing-based estimates was compared with the ground-based information available from the Planning and Development Recovery Committee Task Force of Regional Municipality of Wood Buffalo (RMWB) and National Fire Information Database (NFID); and found strong linear relationships (i.e., r^2-value of 0.97 with a slope of 0.97 for the 2016 HRF over Fort McMurray; and 378 from satellite image vs. 407 from 378 from satellite image vs. 407 from NFID system for the 2011 Lesser Slave Lake fire). Upon delineating the WUI and its associated buffer zones at 10m, 30m, 50m, 70m and 100m distances; we found existence of vegetation within the 30m buffers from the WUI for all of the damaged structures. In addition, we noticed that the relevant authorities had removed vegetation in some areas between 30m and 70m buffers from the WUI in case of Fort McMurray area, which was proven to be effective in order to protect the structures in the adjacent communities. Furthermore, we mapped the wildland fire-induced vulnerable areas upon considering the WUI and its associated buffers. We found that there were still some communities that had the existence of vegetation within the buffer zones; thus such vegetation should be removed and monitored regularly in order to reduce the wildland fire-induced risks.

Introduction

Wildland/forest fire is one of the critical natural hazards that pose a significant threat to the communities located in the vicinity of forested/vegetated areas around the world [1–3]. These fires, in fact, have an enormous impact on the urban/built environment adjacent to the wildland-urban interface (WUI). Those include (i) interruption of usual activities of the residents, (ii) destruction of buildings and other infrastructures, (iii) evacuation of people, (iv) degradation of air quality, and (v) psychological traumatization of the people, among others. In the Canadian context, such fires' impact 20 urban communities, 70,000 people, and forced to evacuate about 8,500 people on an average per annum [4]. In fact, some of the largest wildland fires were occurred in the Western Canada (i.e., in the province of Alberta). For example, Lesser Slave Lake fire in 2011 (also known as the flat top complex fires) caused significant damages (that include the destruction of 510 structures and evacuation of 15,000 residents [5] worth of approximately $750 million [4]. More recently, on 1 May 2016, an enormous wildland fire in Fort McMurray (known as the Horse River Fire, HRF) destroyed 2,579 dwelling units (1,595 structures) and forced to evacuate 88,000 people from the community [6]. Due to this fire event, the total estimated economic impact was about $8.9

billion, which was the costliest insured natural disaster in the Canadian history [7]. In addition, Canada has observed an increasing trend in both the number of evacuations and evacuees as a result of the wildland fires occurred within the WUI over the period 1980-2014 [4]. Moreover, these numbers may potentially increase in the face of climate change [4]. Thus, it is critical for us to study the wildland fire-induced risk at the community level in order to formulate strategies to combat the adverse impacts.

In comprehending the wildland fire-induce risks, one of the most important components is the characterization of the WUI. The detail information required for the appropriate characterization depends on the scale-level of the WUIs, which eventually determine the effectiveness of the risk analysis [8]. In most of the instances, it is a common practice to delineate the WUIs at coarser scales, such as country, regional, and continental levels [8]. In fact, such coarser scale WUIs suffer from several issues [8–10], such as: (i) contain sharp boundaries, (ii) the edges of the classified land cover (including, urban, vegetations, and non-fuels) end abruptly, and (iii) fuels available inside the urban areas are not considered. Therefore, the adoption of these coarser-scale WUIs is relatively less useful for community-level analysis [8,11,12], while they are the top-most impacted stakeholders in the event of an actual fire occurrence. Consequently, it is critical to generate the WUIs at finer scales (i.e., municipal, local, and community levels), which can potentially emphasize on fuel and wildfire hazard management issues at a micro level for the communities. In such cases, the most effective and accurate method is the employment of traditional ground survey; however, it is not only very expensive, but also time-consuming, and a laborious process. In this context, one of the viable alternates may be the use of high spatial-resolution (greater than 2m) optical remote sensing-derived imagery, which is a very much cost-effective, time-saving, and readily available technology.

In order to perceive wildland fire-induced risk at the community level, the comprehension of the damages within the WUI that took place during the historical wildfire events is essential. Such understanding would enable us to identify the connection of the inside urban fuels in the finer-scale WUI that helped to propagate the wildland fire towards the properties/structures. Additionally, this would help us to analyse the presence of wildland fuels in the vicinity of the WUI. In the scope of damage assessment, there are several methods, such as, traditional ground survey-, air-borne remote sensing-, and space-borne remote sensing-based methods. Although the traditional survey method can provide the most detailed and accurate assessment, it suffers similar limitations as described in the previous section for mapping WUI. The second method is the use the air-borne remote sensing that includes the aerial photography, and unmanned aerial vehicle (UAV)-based photography. Some of the such noteworthy case studies included: (i) the Regional Municipality of Wood Buffalo (RMWB) [13] in Alberta, Canada employed aerial-based photographs known as Pictometry imagery taken from five different views (i.e., east, west, north, south, and top) for the Fire Assessment Tool (FAT) to assess the damages occurred due to the HRF in the Fort McMurray urban service area in 2016; (ii) Galarreta et al. [14] analysed UAV imageries of Grounau (Germany), Enschede (the Netherlands), and Bologna (Italy) for urban structural damage assessment. They used oblique imagery taken from multi-angles and 3D point-clouds to develop an automatic damage assessment tool/procedure upon implementing object-based image analysis and semantic reasoning. The study delineated damages related to facades and roofs with aggregated damage score and certainty-measurements; and (iii) Pham et al. [15] combined aerial photographs with LiDAR (Light Detection and Ranging) data to map structural damages in 2010 at Haiti. In reality, the use of air-borne technology has the advantages of proving very high spatial-resolution (usually higher than 0.3m) imagery that facilitates assessing detailed damages of each individual structure. However, the acquisition and processing of such aerial imagery are quite costly, and time-consuming procedure.

In order to overcome the limitations of air-borne remote sensing, space-borne remote sensing (i.e., satellite imagery) can be used in minimizing the cost associated with the image acquisition, and reducing the time for information extraction. Some of the example case-studies include: (i) United Nations High Commissioner for Refugees [16] observed a massive fire destruction in Myanmar using WorldView satellite platforms with a spatial resolution of 0.3 to 0.5m. Their study determined that 275 towns and villages were destroyed or otherwise damaged by fire in Buthidaung, Maungdaw, and Rathedaung Townships in the Maungdaw and Sittwe districts of Rakhine State; (ii) Ehrlich et al. [17] assessed the damages in Wenchuan, China by employing both very high resolution (VHR) optical satellite imageries (i.e., EROS-B, WorldView-1, and SPOT-5) and SAR satellite imageries (i.e., CosmoSkymed and TerraSAR-X). They demonstrated the effectiveness of using such imagery for quantifying building stock and assessing damages; and (iii) Al-Khudhairy et al. [18] employed pan-sharpened IKONOS imagery with a spatial resolution of 1m to quantify the structural damages in the Former Yugoslav Republic of Macedonia, and Jenin-West Bank in the Palestinian territories.

Objectives

In the scope of this report, our overall goal was to use very high spatial resolution (0.5-2.4m) satellite images to develop wildland fire-induced risk framework. We considered two extreme fire events, such as the 2016 HRF over Fort McMurray, and 2011 Lesser Slave Lake fire in Alberta. There were two specific objectives. Firstly, we estimated the number of structural damages due to the wildland fire of interest by using high spatial resolution satellite images, and compared them against ground-based information available from the Planning and Development Recovery Committee Task Force of RMWB, and National Fire Information Database (NFID). Secondly, we delineated the finer resolution WUI using the satellite images, and generated buffer zones at 10m, 30m, 50m, 70m and 100m from the WUI. Subsequently, we used them in quantifying their impacts in damaging the structures and formulating risk zonation induced by the wildland fire at the community-scale.

Note that the main report emphasised on the 2016 HRF over Fort McMurray due to its highest impact in the known Canadian history. On the hand, we included the details of the 2011 Lesser Slave Lake fire in Appendix.

Study Area and Data Requirements

GENERAL DESCRIPTION OF THE STUDY AREA (FORT MCMURRAY REGION)

We considered Fort McMurray as our study area (Figure 1), which is a self-contained 'urban service area' located on the banks of the Athabasca River in the northeastern part of Alberta, Canada. This service area is situated at a distance of approximately 450 km northeast from the nearest metropolitan city Edmonton. The population of Fort McMurray is approximately 66,573 [19], which has grown significantly (i.e., from 1,186 to 61,374) over the period 1961-2011 [20]. Such population growth has been observed as a result of developing oil sands resources in the Greater Athabasca Region. This region, in fact, is the third largest confirmed oil deposits in the world; and covers an area of approximately 140,000 km^2 [21]. Being the center of the oil sands industry, Fort McMurray dominates the local to national economy that contributes to the 30% of the total regional labor force [22].

The climate of Fort McMurray is considered as severe during winters, and mild to warm and dry summers for only three months. The daily average temperature in January and July for the Fort McMurray during 1981-2010 were recorded -17.4 and +17.1 ^{o}C, respectively [23]. The region is characterized by a borderline subarctic climate, which is very close to the humid continental climate. The annual average precipitation of the area is 418.6 mm during the 1981-2010 period [23]. The physiography of the area is considered as 'Northern Alberta Lowlands' [24], which is having an average elevation of 369 meter above mean sea level [25]. The area falls under the 'Central Mixedwood' natural subregions of Alberta [24], which is surrounded by thick boreal forest with a mix of bog and oil sands with dense coniferous covering [26]. Due to the presence of hefty boreal forest coupled with drier summer, the 'Central Mixedwood' natural subregion has experienced significant amount of wildland fires, i.e., 9,323 number of lightning-caused and 9,101 number of human-caused fires; which constituted as approximately 34.37% of the total wildland fire incidents in Alberta during the 1961-2014 period [27].

FIGURE 1: THE SPATIAL EXTENT OF THE STUDY AREA HIGHLIGHTING THE 'FORT MCMURRAY URBAN SERVICE AREA' AND COMMUNITY BOUNDARIES USING SOLID AND DOTTED POLYGONS RESPECTIVELY USING A WORLDVIEW-2 SATELLITE IMAGE ACQUIRED ON 06 JUNE 2016; WHICH IS LOCATED IN THE NORTHEASTERN PART OF THE PROVINCE OF ALBERTA. NOTE THAT THE URBAN AREA IS SURROUNDED BY BOTH BURNED (AS SEEN IN DARK GREENISH TO GRAY COLORS) AND HEALTHY (BRIGHT RED TO REDDISH COLORS) VEGETATION.

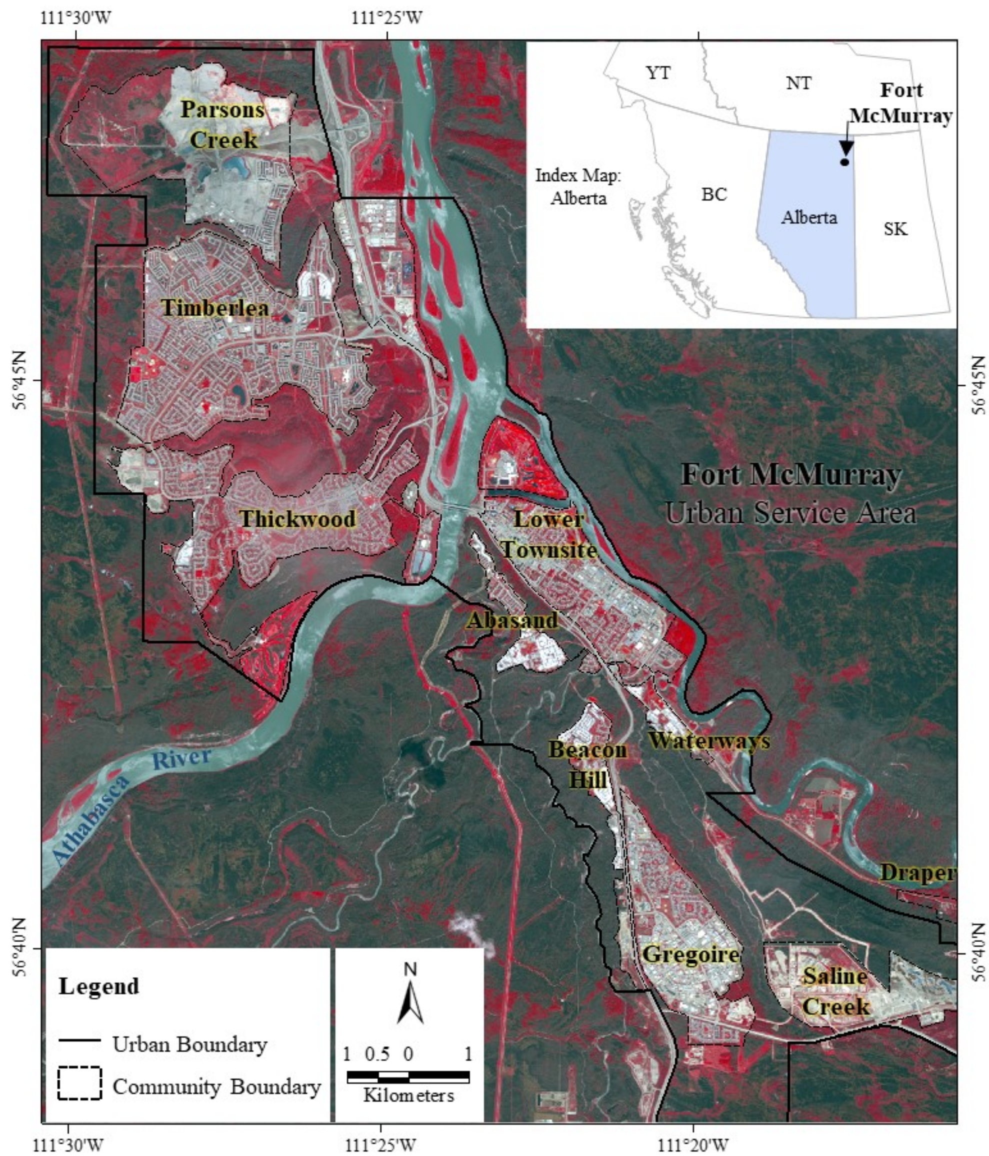

DATA REQUIREMENTS

In this study, we primarily used three key datasets, such as: (i) space-borne WorldView-2 satellite imagery received from DigitalGlobe Foundation, (ii) historical imageries available from Google Earth Pro system, and (iii) statistical ground data of the damaged structures from RMWB after the fire event in 2016. In case of the WorldView-2 imagery, it was acquired on 06 June 2016 (i.e., post wildland fire event) in both panchromatic (Pan, spatial resolution 0.5m) and multispectral (MS, spatial resolution 2.0m) modes. The Pan band of WorldView-2 covers spectral wavelengths of 0.45-0.80 µm. In contrast, the WorldView-2 MS provides eight multispectral bands that includes, coastal (0.40-0.45 µm), blue (0.45-0.51 µm), green (0.51-0.58 µm), yellow (0.585-0.625 µm), red (0.63-0.69 µm), red edge (0.705-0.745 µm), near infrared-1 (0.77-0.895 µm), and near infrared-2 (0.86-0.90 µm) [28]. However, we employed four MS bands (i.e., blue, green, red, and near infrared-1) for mapping and assessing structural-damages in this study. Whereas, we utilized a combination of Pan and MS coupled with historical imageries of Google Earth Pro for the characterization of WUI and the risk modelling for the pre-during-post events of the wildland-fire in Fort McMurray. In addition, we obtained the ground-based data in relation to the damaged structures; which were gathered and analysed by the RMWB Planning and Development Recovery Committee Task Force, and reported in McIntyre [6]. Furthermore, we acquired additional information from RMWB (Allison Kennedy-Drake, Performance & Risk Analyst of Recovery Task Force; personal communication). Those included: (i) multiple dwelling units or townhouses with a single and continuous rooftop was counted as one structure-loss or multiple structure loss, (ii) a damaged unattached-garage was counted as one structure-loss or not, (iii) a business with multiple structures was considered as multiple count or a single count of loss, etc. We, then, used this information in validating the remote sensing-derived estimates of the damaged structures. Finally, we gathered more information regarding the community street maps, structural plans and Municipal Development Plan of RMWB [29,30], and the community protection guidelines of Canadian FireSmart [31,32]; used them both in delineating community boundaries and modelling risks associated with wildland fire.

Note that we were unable to use the NFID-provided database for the 2016 HRF over Fort McMurray area. Despite, we obtained the wildland fire-induced structural damage information from the RMWB Planning and Development Recovery Committee Task Force; which would be eventually added in the existing NFID system. However, we employed such NFID-provided information in case of studying the 2011 Lesser Slave Lake fire event (please see Appendix for details).

Methods

PRE-PROCESSING OF WORLDVIEW-2 IMAGES

Upon acquiring the WorldView-2 satellite images, we performed the following pre-processing steps on both Pan and MS bands of interest (i.e., blue, green, red, and nearinfrared-1). Those included: (i) converting the digital numbers (DN) of the pixels in the images to radiance values (Eq. 1) [33,34], (ii) transforming the radiance values to surface reflectance values (Eq. 2) [33,35], (iii) re-projecting the images into Universal Traverse Mercator (UTM) Zone 12 N with North American Datum 1983

(NAD 83), and (iv) clipping the images to the extent of the study area. Further, we used this pre-processed dataset in mapping of the spatial dynamics due to the HRF in Fort McMurray area as described in the following sub-section.

$$L_\lambda = G * DN + B \quad (1)$$

$$\rho_\lambda = \frac{\pi * [L_\lambda - L_\lambda(haze)] * d^2}{ESUN_\lambda * \cos\theta_s} \quad (2)$$

where, L_λ and ρ_λ are the radiance and surface reflectance, *DN* is the digital number, *G* and *B* are the gain and bias values, L_λ *(haze)* is the minimum radiance value in the histogram, *d* is Earth-Sun distance in astronomical units, $ESUN_\lambda$ is mean solar exoatmospheric irradiances, and Θ_s is solar zenith angle. All these parameters are band-specific, and the values of *G*, *B*, *d*, $ESUN_\lambda$, and Θ_s are available from the metadata files of the images.

MAPPING OF STRUCTURAL DAMAGES AND OTHER FEATURES

In delineating the features of interest, i.e., “structural damage”, “burned forest/grass”, “non-burned forest” and “non-burned grass” over the study area, we applied ISODATA (i.e., iterative self-organizing data analysis technique) clustering technique to the WorldView-2 MS image. Our preference of using this clustering technique was due to its ability of statistically attributing each and every pixel of an image to generate specific number of classes based on the spectral similarities [36]. In this process, we generated 50 classes with a convergence threshold of 0.995 by assigning an infinite number of iterations. Subsequently, we evaluated the patterns of cluster-specific spectral signatures, and grouped them according to our features of interest.

In case of mapping “structural damage”, we consulted additional datasets, such as historical imageries acquired between August 2015 and May 2016 available from Google Earth Pro and Fire Map of RMWB [13]. At this stage, we appraised a qualitative assessment and noticed few large buildings (mostly with flat rooftops) with no fire-induced damages were misclassified as damaged structures. To address this issue, we defined such areas and applied a decision rule of declaring them as non-damaged structures. Additionally, we observed some scattered misclassified pixels, which were then removed by applying ‘clump’ and ‘eliminate’ functions. Finally, we counted the number of damaged structures, and validated them with the ground-based information synthesized by the RMWB Planning and Development Recovery Committee Task Force [6]. In this case, we determined the degree of agreements between the satellite- and ground-based estimates of structural damages by percentage error at the community-level.

For the “burned forest/grass”, “non-burned forest” and “non-burned grass”, we conferred with the available historical imageries from Google Earth Pro as mentioned above in order to comprehend the vegetation dynamics during the pre-event of HRF. We observed that some burned forest/grass and non-burned forest in the southern portion of the Thickwood neighborhood were misclassified as “non-burned grass”. This was, in fact, due to the presence of haze-effect on that part of the image. Thus, we identified the extent of the haze areas and implemented a decision rule to assign the “non-burned grass” to “burned forest/grass” and “non-burned forest” as appropriate. Additionally, for “non-burned grass”, we recognized that some areas were misclassified as “non-burned forest”. To sort out this issue, we performed a texture analysis, and applied a decision rule to recode the misclassified forest as “non-burned forest” having rough texture, and as “non-burned grass” having smooth texture. We eventually used these three feature-classes in the wildland fire-induced risk zonation and discussed further in the following sub-section.

DELINEATING WUI, RISK ZONATION AND ASSESSMENT

In order to delineate risk zones, and assess the presence/absence of vegetation (i.e., fuels) within these zones, we employed a combination of WorldView-2 Pan and MS data. In this case, we accomplished such integration using a pan-sharpening technique known as subtractive resolution merge [37,38]. In fact, such technique would enhance the visualization, and also allow observing finer details on the pan-sharpened image [39,40]. Note that we did not use this pan-sharpened image for delineating spatial features as detailed in the previous sub-section, because the pan-sharpening would affect the original spectral quality provided by the multispectral bands [41,42].

In delineating the WUI, we visualized the pan-sharpened image at 1:2,000 scale and drew the interface upon considering the property-lines adjacent to the wildland. This finer scale ratio, in fact, aided visualizing spatial features in such a detail, which was not possible using the Community Street Maps of Fort McMurray available at 1:10,000 scale [29]. It would be worthwhile to mention that we delineated structure- or building-based WUI, which would be a common practice for mapping finer scale WUI from high resolution imagery [43,44]. Next, we generated three outside-buffers of 10m, 30m, and 100m from the WUI, which were the Interface Priority Zones (IPZ) described in the guidebook for community Protection of FireSmart Canada [32,45] for managing vegetation around WUI. Upon generating the buffers, we assessed the presence of different fuels (i.e., forest and grass in particular) and their on-ground standing arrangements (i.e., clear-cut, thinning, and pruning) within each of the buffer zone for three different time-frames, i.e., before, during, and after the HRF. At this stage, we consulted with the historical imageries acquired between August 2015 and May 2016 available from Google Earth Pro for the assessment of standing-vegetation that potentially posed risk for the communities before and during the wildland fire event. During the aftermath of the fire event, we used the spatial features (that included “structural damage”, “burned forest/grass”, “non-burned forest” and “non-burned grass”) as described in the previous sub-section. While assessing the risks for the three buffer-zones, we perceived that additional buffer zones would be very useful for assessing potential risks at the community level. Hence, we generated additional two buffer zones from the WUI, i.e., 50m and 70m for providing recommendations in order to reduce the wildland fire-induced risks for the communities in the study area.

Results and Discussion

STRUCTURAL DAMAGE ASSESSMENT

Figure 2 shows the WorldView-2 MS derived structural damages, including other features, i.e., burned forest/grass, non-burned forest and non-burned grass over the communities of the study area. We found that the highest number of structural damages occurred in the communities of Beacon Hill (411 structures), and Abasand (359 structures). In contrast, we estimated that the lowest structural damage took place in the community of Lower Townsite (1 structure), which was followed by Gregoire (3 structures) and Parsons Creek (8 structures). We compared the number of structural damages derived from our proposed method with the ground-based estimates at the community level (Figure 3). Note that we considered only eight communities (i.e., Abasand, Beacon Hill, Gregoire, Lower Townsite, Parsons Creek, Thickwood, Timberlea, and Waterways), which were completely covered by the satellite image. However, we were unable to estimate such damages over other communities within the Wood Buffalo Region, because those areas were either covered partially (e.g., Draper, and Saline Creek) or not at all (e.g., Anzac, Saprae Creek, and Fort McMurray International Airport) by the satellite image. In general, we observed a very good relationship (i.e, $r^2 = 0.97$ with a slope and intercept of 0.97 and 1.53, respectively) between satellite-based remote sensing and ground-based estimates. In most of the cases, our estimates were either at par or slightly below except for the community of Abasand. The probable rationales of such under estimates were as follows:

- The satellite image provided only the top view, i.e., rooftops of the structures; which was unable to provide any further information related to damages occurred in the side-walls of the structures. As a result, we failed to identify such damaged structures.
- In the areas with the presence of both large and small houses together (e.g., Beacon Hill North, Beacon Hill South, and Waterways), it would be possible that we counted few small houses as detached garages. Also, note that we didn't count the damaged detached garages as separate structures, rather than included as part of the main structures.
- In case of the community of Beacon Hill, our count difference was the highest (i.e., ground-based estimates of 447 vs. remote sensing-based estimates of 411). In addition to the above-mentioned causes, there might have another reason. In the southern part of the community (i.e., Centennial RV Park at around the Latitude 56° 40′ 47′′ N and Longitude 111° 21′ 13′′ W), we observed an informal arrangement of several damaged structures, which were probably a campground having temporary shelters of tiny and linear houses, trucks, or caravans. In this case, we did not include those small damages in our estimates, rather counted only the two permanent structures located in the area.

Note that we also found two damaged structures in Dickinsfield (near the intersection of McConachie Crescent and Clenell Crescent) of the Thickwood community, which were burned after the HRF event. Thus, we didn't include them in our count of fire-induced structural damages.

In addition, in the community of Abasand, we had over estimations, i.e., ground-based estimates of 347 vs. remote sensing-based estimates of 359. It might be attributed due to the following reasons:

- We might have counted some detached garage as separate structure in the dense built-up locations, where the boundaries of the houses were not clearly distinguishable from the satellite image;
- It would be quite possible that some of the town-houses were continuous. However, we were unable to identify such connectivity; thus, interpreted and counted as separate structures; and
- Since it would be quite challenging to comprehend the utilization of the structures from the satellite data, so that a business with multiple structures would possibly be counted as multiple structural damages. Note that one business operation with several structures were considered as one structure in the ground-based estimates (Allison Kennedy-Drake, Performance & Risk Analyst of Recovery Task Force; personal communication).

FIGURE 2: THE SPATIAL EXTENT OF THE STRUCTURAL DAMAGE DERIVED FROM WORLDVIEW-2 MS SATELLITE IMAGE INCLUDING OTHER SPATIAL FEATURES OF INTEREST.

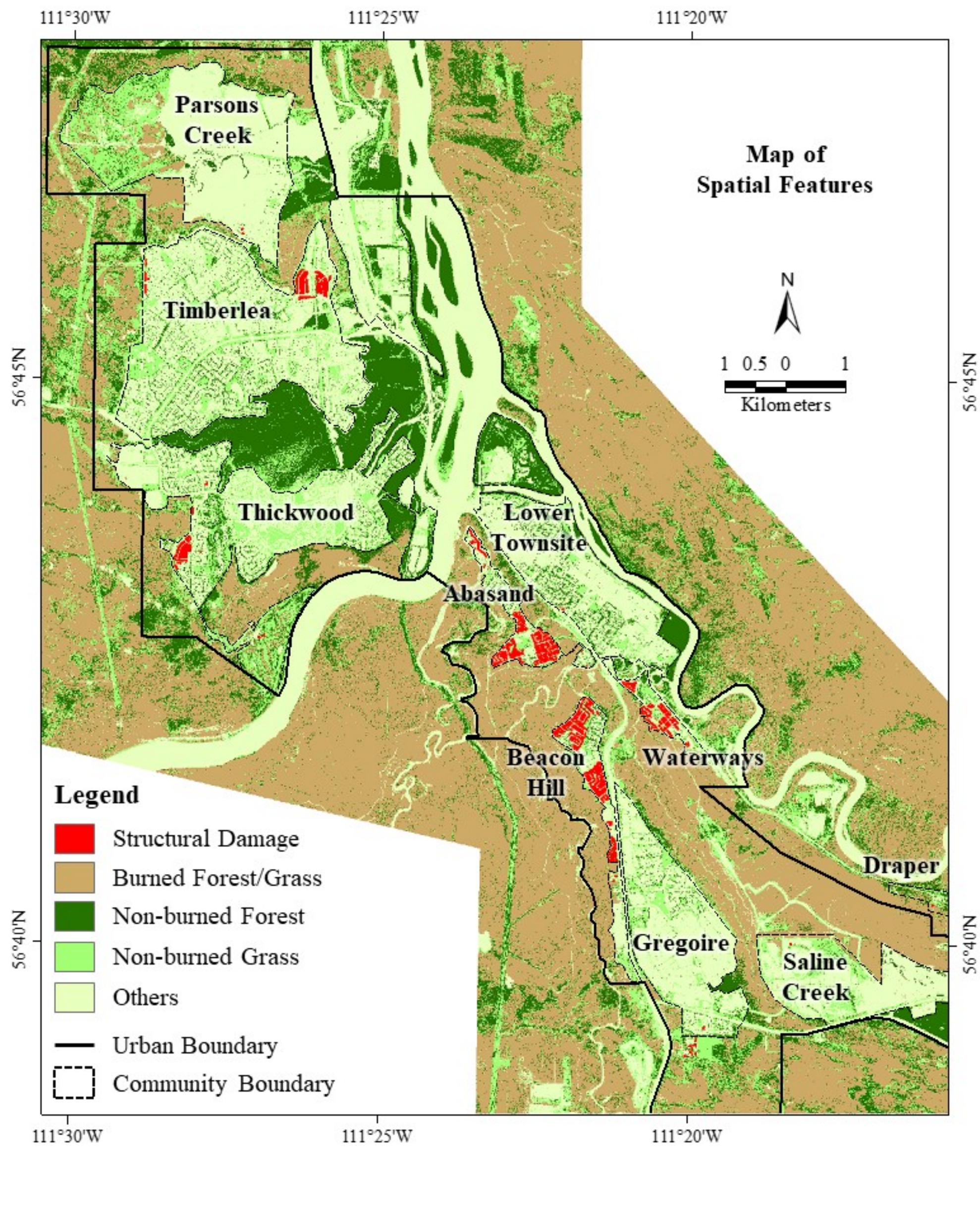

FIGURE 3: RELATIONSHIPS BETWEEN THE STRUCTURAL DAMAGE ESTIMATES USING SATELLITE- AND GROUND-BASED COUNTS.

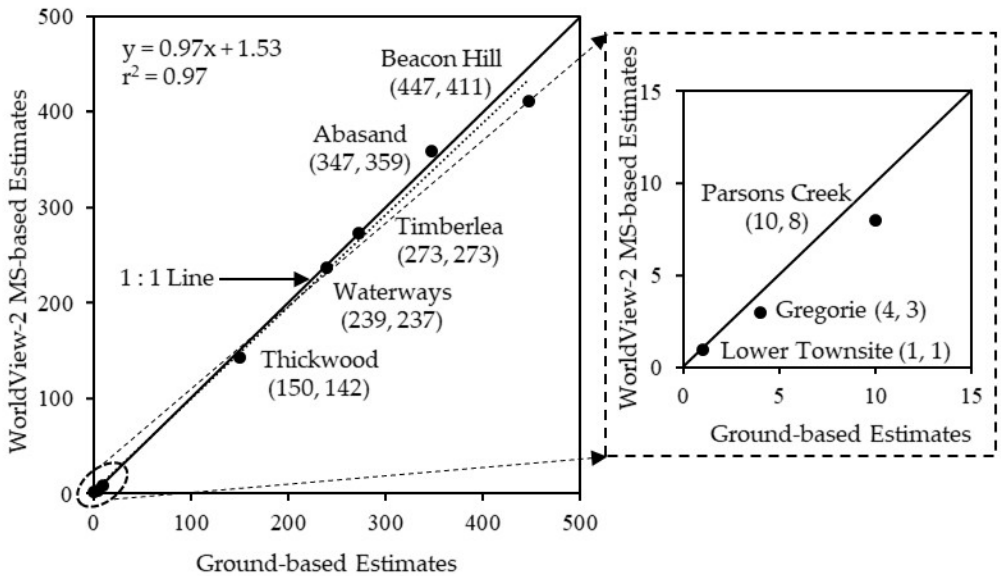

DELINEATION OF WUI AND BUFFERS, AND ASSESSMENT OF POTENTIAL RISKS

As per the methods discussed in the sub-section "mapping of structural damages and other features" under "Methods", we contrived the WUI and its associated buffers at 10m, 30m, 50m, 70m, and 100m. Subsequently, we investigated two specific issues, i.e., (i) relation with the WUI and its associated buffers and fire-induced structural damages, (ii) delineation of the spatial dynamics of the wildland fire-induced vulnerable area. In case of the areas with observed structural damages, we found that there was presence of vegetation (fuel for the fire; see Figure 2 for burned forest/grass, and non-burned forest and grass) within the 10m buffer from the WUI in most of the instances (see Figure 4a,b for example cases). Furthermore, we noticed the existence of vegetation within the next 20m from the 10m buffer (i.e., 30m buffer from the WUI) for the remaining areas of structural damages (see Figure 4c,d for example cases). Thus, we might infer that the zone of 30m buffer should have very little to no existence of vegetation in order to avoid the propagation of wildland fire into the communities.

FIGURE 4: EXAMPLES OF AREAS OF WILDLAND FIRE-INDUCED STRUCTURAL DAMAGES WHERE THERE WAS PRESENCE OF VEGETATION (FUEL FOR FIRE PROPAGATION) WITHIN 10M (PANELS A & B) AND 30M (PANELS C & D) BUFFERS FROM THE WUI.

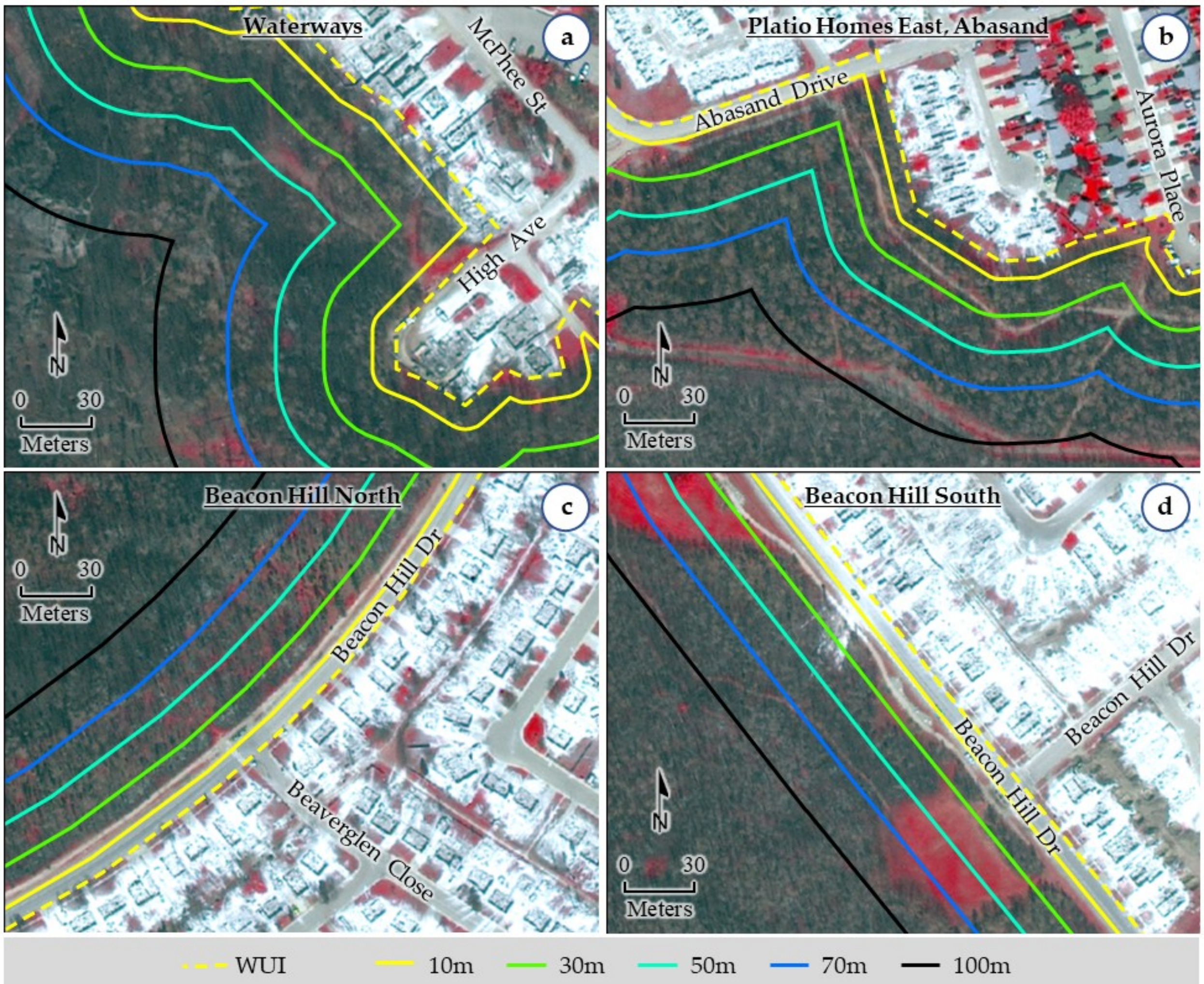

It would be interesting to note that we observed the removal of vegetation between 30m and 70m buffers from the WUI (see Figure 5 for an example). In fact, we assumed that such operation was carried out by relevant authorities in order to protect the structures in the nearby communities; which was evident upon consulting very high spatial resolution satellite imageries available from Google Earth Pro acquired on 03, 04, 05, 07, and 12 May 2016. From this observation, we might emphasis that a vegetation zone of up to 70m from the WUI would enhance the safety measures in order to reduce the wildland fire-induced risk. Thus, our delineation of additional buffer zones of 50m and 70m from the WUI would be effective and helpful in formulating better wildland fire-induce risk mitigation strategies. In addition, we also looked into the wildland fire-induced vulnerable areas upon considering the WUI and its associated buffers. We found that there were still some communities that had the existence of vegetation within the buffer zones (see an example in Figure 5c). In such circumstances, we would recommend that the vegetation should be removed. Also, in order to reduce the wildland fire-induced risks, it would be critical to have a regular monitoring system in place to assess the vegetation conditions and remove them if deemed necessary.

FIGURE 5: EXAMPLE OF AREAS WITH GUIDED VEGETATION REMOVAL IN ORDER TO PROTECT NEARBY COMMUNITIES SUCH AS TIMBERLEA AND PARSONS CREEK IN PARTICULAR. PANEL (C) SHOWS AN EXAMPLE OF WILDLAND FIRE-INDUCED VULNERABLE AREA. ALSO, THE LAYOUT OF THE SYNCRUDE ATHLETIC PARK PROVIDES PROTECTION TO THE NEARBY COMMUNITY FROM THE PROPAGATION OF WILDLAND FIRES [PANEL (A)].

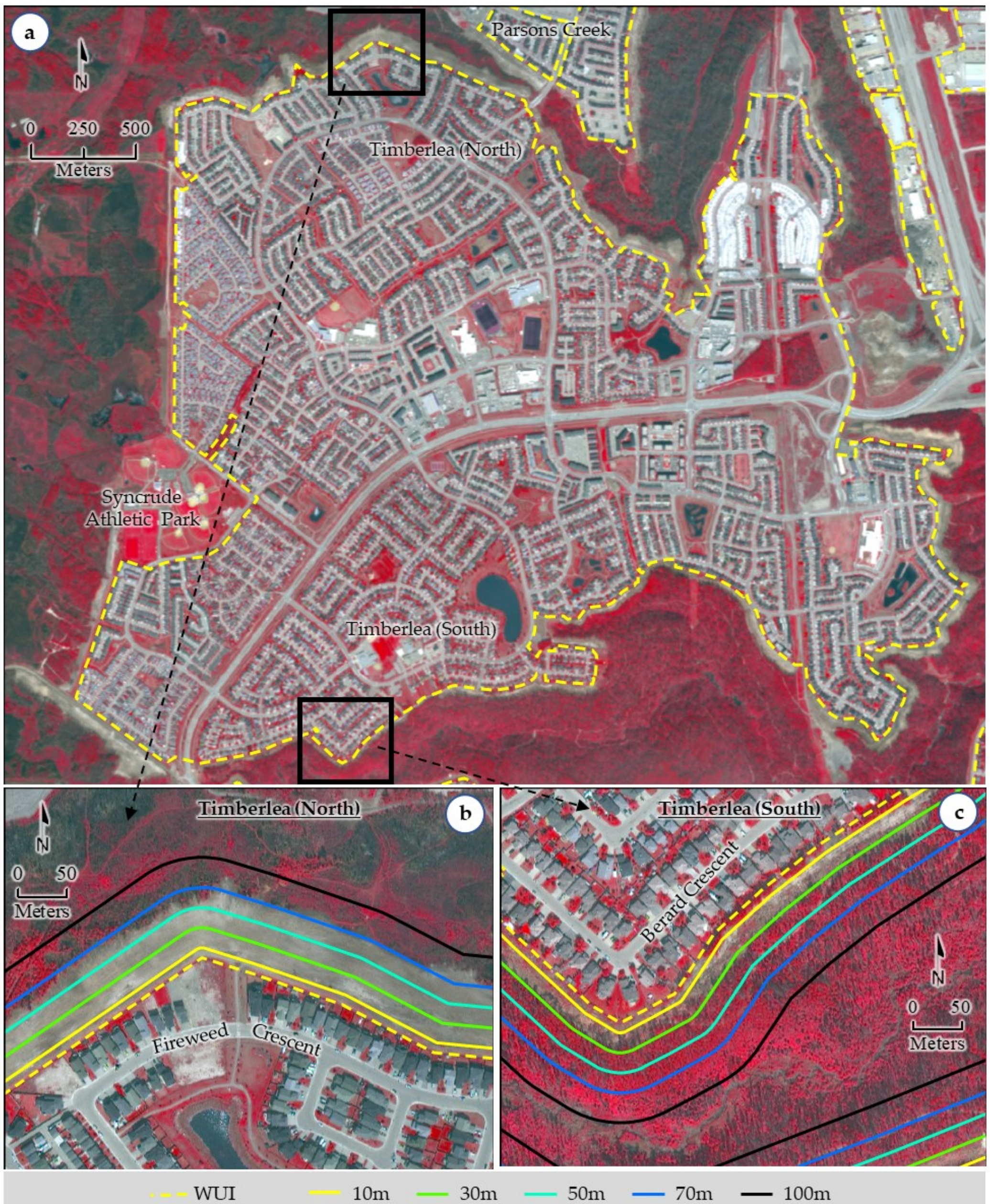

OTHER CONSIDERATIONS

Apart from the delineation of structural damages in communities and assessment of vulnerabilities due to the HRF, we also summarized a few interesting evidences while evaluating the developed models and risk zonation (i.e., buffers in this particular case). In case of Syncrude Athletic Park, we discerned that the area was situated at the western part of Timberlea community (Figure 5a). There were some fuel connections to expand the wildland fire into the Athletic Park's compound and so did towards the nearest community. However, due to having some open space with very little vegetation, wildland fire did not spread out to other communities; where the Atheltetic Park itself worked as a major obstacle to fire propagation. Through this experience, we assumed that similar major social service infrastructures (e.g., Elementary Schools); recreation activities (Athletic Parks, Golf Courses); shopping malls (e.g., Walmart, Canadian Tier), and major highways (wider than 40m including the right of ways) could be planned at the outskirts of the urban service area to create fuel-break in future development. We also would suggest that considerations should be given priority to erect the parking lots for shopping malls, playgrounds, churches, golf courses, schools, etc. that would fetch the vegetated areas as a major barrier for wildland fire spread. Also, we would like to suggest that the land use plans should incorporate the wildland fire-vulnerability information if not included in the current practice.

Concluding Remarks

In the scope of this report, we demonstrated the effectiveness of using Worldview-2 in developing a wildland fire-induced risk modelling framework and applied for the comprehension of the 2016 HRF occurrence in Fort McMurray, Alberta. We found that the estimates of the fire-induced structural damages using satellite- and ground-based information exhibited strong linear relations, i.e., r^2-value of 0.97 with a slope of 0.97. We also observed that vegetation was available within the 10 to 30m buffers from the WUI, which thought to be the reason of the propagation of the fire and reasonable for the structural damages. Furthermore, our consultation with the very high spatial resolution satellite images available from the Google Earth Pro acquired between 03 and 12 May 2016 (that coincided with the HRF duration) revealed that the relevant authorities had removed vegetation in some critical areas between 30 and 70 m buffers in order to protect the structures in the nearby communities. Also, upon mapping the wildland fire-induced vulnerable areas using the WUI and its associated buffers, we spotted that the existence of vegetation within the 10 to 30m buffer zones around some communities, which would be removed the wildland fire-induced risks. Despite our findings, we strongly recommend that our proposed methods should be carefully evaluated and modified accordingly (if deemed necessary) prior to adopting in other ecosystems.

References

1. Thomas, D.S.; Butry, D.T. Wildland fires within municipal jurisdictions. *J. For.* **2012**, *110*, 34–41, doi:10.5849/jof.10-024.
2. Haynes, H.; Garcia, A.; Madsen, R. *Wildland/Urban Interface: Fire Department Wildfire Preparedness and Readiness Capabilities*, Phase One Report; National Fire Protection Association: Quincy, MA, 2015.
3. Tedim, F.; Xanthopoulos, G.; Leone, V. Forest fires in Europe: facts and challenges. *Wildfire Hazards, Risks, and Disasters* **2015**, 77–99, doi:10.1016/B978-0-12-410434-1.00005-1.
4. Natural Resources Canada: Wildland fire evacuations. Available online: http://www.nrcan.gc.ca/forests/climate-change/forest-change/17787 (accessed on 08 November 2017).
5. Alberta Emergency Management Agency. *Alberta Wildland / Urban Interface Fires: A Guide for Municipal Directors of Emergency Management and Consequence Management Officers*; Government of Alberta: Edmonton, Alberta, Canada, 2015.
6. McIntyre, J. *Moving forward: The Economic Impact of Rebuilding the Wood Buffalo Region's Economy*; The Conference Board of Canada: Ottawa, Ontario, Canada, 2017.
7. KPMG. *May 2016 Wood Buffalo Wildfire: Post-Incident Assessment Report, Final Report*; KPMG LLP: Switzerland, 2017.
8. Whitman, E.; Rapaport, E.; Sherren, K. Modeling fire susceptibility to delineate wildland-urban interface for municipal-scale fire risk management. *Environ. Manage.* **2013**, *52*, 1427–1439, doi:10.1007/s00267-013-0159-9.
9. Stewart, S.I.; Radeloff, V.C.; Hammer, R.B.; Hawbaker, T.J. Defining the wildland – urban interface. *J. For.* **2007**, *105*, 201–207.
10. Modugno, S.; Balzter, H.; Cole, B.; Borrelli, P. Mapping regional patterns of large forest fires in Wildland-Urban Interface areas in Europe. *J. Environ. Manage.* **2016**, *172*, 112–126, doi:10.1016/j.jenvman.2016.02.013.
11. Radeloff, V.C.; Hammer, R.B.; Stewart, S.I.; Fried, J.S.; Holcomb, S.S.; McKeefry, J.F. The wildland-urban interface in the United States. *Ecol. Appl.* **2005**, *15*, 799–805, doi:10.1890/04-1413.
12. Theobald, D.M.; Romme, W.H. Expansion of the US wildland-urban interface. *Landsc. Urban Plan.* **2007**, *83*, 340–354, doi:10.1016/j.landurbplan.2007.06.002.
13. Regional Municipality of Wood Buffalo: Fire Assessment Tool. Available online: http://firemap.rmwb.ca/ (accessed on 16 November 2017).
14. Galarreta, J.F.; Kerle, N.; Gerke, M. UAV-based urban structural damage assessment using object-based image analysis and semantic reasoning. *Nat. Hazards Earth Syst. Sci.* **2015**, *15*, 1087–1101, doi:10.5194/nhess-15-1087-2015.
15. Pham, T.-T.-H.; Apparicio, P.; Gomez, C.; Weber, C.; Mathon, D. Towards a rapid automatic detection of building damage using remote sensing for disaster management. *Disaster Prev. Manag.* **2014**, *23*, 53–66, doi:10.1108/DPM-12-2012-0148.
16. United Nations High Commissioner for Refugees: Destroyed areas in Buthidaung, Maungdaw, and Rathedaung Townships of Rakhine State in Myanmar. Available online: http://www.unitar.org/unosat/

node/44/2727?utm_source=unosat-unitar&utm_medium=rss&utm_campaign=maps (accessed on 17 November 2017).
17. Ehrlich, D.; Guo, H.D.; Molch, K.; Ma, J.W.; Pesaresi, M. Identifying damage caused by the 2008 wenchuan earthquake from VHR remote sensing data. *Int. J. Digit. Earth* **2009**, *2*, 309–326, doi:10.1080/17538940902767401.
18. Al-Khudhairy, D.H.A.; Caravaggi, I.; Glada, S. Structural damage assessments from Ikonos data using change detection, object-oriented segmentation, and classification techniques. *Photogramm. Eng. Remote Sensing* **2005**, *71*, 825–837, doi:10.14358/PERS.71.7.825.
19. Statistics Canada: Census Profile, 2016 Census. Available online: http://www12.statcan.gc.ca/census-recensement/2016/dp-pd/prof/details/page.cfm?Lang=E&Geo1=POPC&Code1=0292&Geo2=PR&Code2=47&Data=Count&SearchText=FortMcMurray&SearchType=Begins&SearchPR=01&B1=All&wbdisable=true (accessed on 21 November 2017).
20. Rahaman, K.R.; Hassan, Q.K. Quantification of local warming trend: A remote sensing-based approach. *PLoS One* **2017**, *12*, 1–18, doi:10.1371/journal.pone.0169423.
21. Papineau, J.W.; Deacon, L. Fort McMurray and the Canadian oil sands: local coverage of national importance. *Environ. Commun.* **2017**, *11*, 593–608, doi:10.1080/17524032.2017.1289107.
22. Long Range Planning and Policy, RMWB. *Envision Wood Buffalo Towards 250k: Fort McMurray - Where We are Today*; Regional Municipality of Wood Buffalo: Fort McMurray, Alberta, 2008.
23. Environment Canada: Canadian Climate Normals 1981-2010 Station Data. Available online: http://climate.weather.gc.ca/climate_normals/results_1981_2010_e.html?stnID=367&autofwd=1 (accessed on 22 November 2017).
24. Natural Regions Committee. *Natural Regions and Subregions of Alberta*; Compiled by D.J. Downing and W.W. Pettapiece; Government of Alberta: Edmonton, Alberta, Canada, 2006.
25. Girardin, M.P.; Wotton, B.M. Summer moisture and wildfire risks across Canada. *J. Appl. Meteorol. Climatol.* **2009**, *48*, 517–533, doi:10.1175/2008JAMC1996.1.
26. Stirling, M. Fort McMurray wildfire 2016: Conflating human-caused wildfires with human-caused global warming. *Soc. Sci. Res. Netw.* **2017**, doi:10.3386/w19846.
27. Alberta Wildfire: Historical Wildfire Database. Available online: http://wildfire.alberta.ca/resources/historical-data/historical-wildfire-database.aspx (accessed on 22 November 2017).
28. Satellite Imaging Corporation: WorldView-2 Satellite Sensor. Available online: https://www.satimagingcorp.com/satellite-sensors/worldview-2/ (accessed on 21 November 2017).
29. Regional Municipality of Wood Buffalo: Community Street Maps. Available online: https://www.rmwb.ca/living/Maps/Community-Street-Maps.htm (accessed on 06 November 2017).
30. Regional Municipality of Wood Buffalo. *Municipal Develoment Plan, Bylaw No. 11/027*; RMWB, Alberta, 2011.
31. Patners in Protection. *FireSmart: Protecting Your Community from Wildfire*; Maryhelen Vicars & Associates, Eds.; 2nd Ed.; Edmonton, Alberta, Canada, 2003.

32. Alberta Government. *FireSmart: Guidebook for Community Protection. A Guidebook for Wildland/Urban Interface Communities*; Provincial Forest Fire Centre: Edmonton, Alberta, Canada, 2013; ISBN 9781460107805.
33. Chávez, P.S.J. Image-based atmospheric corrections - revisited and improved. *Photogramm. Eng. Remote Sensing* **1996**, *62*, 1025–1036, doi:0099-1112/96/6209-1025.
34. Hoang, T.C.; O'Leary, M.J.; Fotedar, R.K. Remote-sensed mapping of *Sargassum* spp. distribution around Rottnest Island, Western Australia, using high-spatial resolution WorldView-2 satellite data. *J. Coast. Res.* **2016**, *322*, 1310–1321, doi:10.2112/JCOASTRES-D-15-00077.1.
35. Nazeer, M.; Nichol, J.E.; Yung, Y.K. Evaluation of atmospheric correction models and Landsat surface reflectance product in an urban coastal environment. *Int. J. Remote Sens.* **2014**, *35*, 6271–6291,doi:10.1080/01431161.2014.951742.
36. Lillesand, T.M.; Kiefer, R.W.; Chipman, J.W. *Remote Sensing and Image Interpretation,* 5th Ed.; John Wiley & Sons Inc.: New York, USA, 2004; ISBN:0470052457.
37. Ashraf, S.; Brabyn, L.; Hicks, B.J. Introducing contrast and luminance normalisation to improve the quality of subtractive resolution merge technique. *Int. J. Image Data Fusion* **2013**, *4*, 230–251,doi:10.1080/19479832.2013.782072.
38. Zhang, Y.; Mishra, R. A review and comparison of commercially available pan-sharpening techniques for high resolution satellite image fusion. In Geoscience and Remote Sensing Symposium (IGARSS), 2012 IEEE International, Munich, Germany, 22-27 July 2012; IEEE; 182–185.
39. Jovanović, D.; Govedarica, M.; Sabo, F.; Važić, R.; Popović, D. Impact analysis of pansharpening Landsat ETM+, Landsat OLI, WorldView-2, and Ikonos images on vegetation indices. In Procceedings of the Fourth International Conference on Remote Sensing and Geoinformation of the Environment (RSCy2016), Paphos, Cyprus, 12 August 2016; International Society for Optics and Photonics; vol.9688, p. 968814.
40. Rahaman, K.R.; Hassan, Q.K.; Ahmed, M.R. Pan-sharpening of Landsat-8 images and its application in calculating vegetation greenness and canopy water contents. *ISPRS Int. J. Geo-Information* **2017**, *6*, 168, doi:10.3390/ijgi6060168.
41. Chavez, P.S. Comparison of spatial variability in visible and near-infrared spectral images. *Photogramm. Eng. Remote Sensing* **1992**, *58*, 957–964.
42. Johnson, B. Effects of pansharpening on vegetation indices. *ISPRS Int. J. Geo-Information* **2014**, *3*, 507–522, doi:10.3390/ijgi3020507.
43. Caggiano, M.D.; Tinkham, W.T.; Hoffman, C.; Cheng, A.S.; Hawbaker, T.J. High resolution mapping of development in the wildland-urban interface using object based image extraction. *Heliyon* **2016**, *2*, e00174, doi:10.1016/j.heliyon.2016.e00174.
44. Lowell, K.; Shamir, R.; Siqueira, A.; White, J.; O'Connor, A.; Butcher, G.; Garvey, M.; Niven, M. Assessing the capabilities of geospatial data to map built structures and evaluate their bushfire threat. *Int. J. Wildl. Fire* **2009**, *18*, 1010–1020, doi:10.1071/WF08077.
45. The BC Forest Service. *The Home Owners FireSmart Manual: Protect your home from wildfire (B.C. Edition)*; British Columbia, Canada, 2003.

Acknowledgements

This project is supported by the Canadian Safety and Security Program, a federal program led by Defence Research and Development Canada's Centre for Security Science, in partnership with Public Safety Canada. Partners in the project include the Canadian Association of Fire Chiefs (CAFC), the Council of Canadian Fire Marshals and Fire Commissioners (CCFMFC), Public Safety Canada, and Rhapsody Strategies Inc. Additionally, the WorldView-2 image used in this project is provided in the form of an “imagery grant” by the DigitalGlobe Foundation; and the ground-based estimates in relation to the structural damages are available from: (i) the Planning and Development Recovery Committee Task Force of Regional Municipality of Wood Buffalo (RMWB) for the 2016 HRF event over Fort McMurray; and (ii) NFID-provided information for the 2011 Lesser Slave Lake fire event.

Author Biographical Information

Dr. Quazi K. Hassan is a professor in the Department of Geomatics Engineering and leads the Earth Observation for Environmental Laboratory. His research interests include: (i) application of remote sensing in forecasting and monitoring of natural hazards/disasters, such as forest fire, drought, and flooding; (ii) use of remote sensing and GIS techniques in understanding the dynamics of natural resources, such as forestry, agriculture, and water; and (iii) integration of remote sensing, GIS, and modelling techniques in addressing issues related to energy, environment, climate change, local/global warming and smart city. He holds research grants from NSERC, Government of Alberta, leading energy industry, and NGOs. Dr. Hassan is currently serving the editorial board of Scientific Reports (Nature Publication Group) and Remote Sensing (MDPI) among others. Email: qhassan@ucalgary.ca

Mr. M. Razu Ahmed is a researcher at the Department of Geomatics Engineering and a member of the Earth Observation for Environment Laboratory. His research interests include: (i) application of remote sensing for environmental modelling; (ii) natural disasters with keen interest in wildland fires; (iii) application of remote sensing and GIS in solving environmental issues; and (iv) modelling vegetation dynamics using remote sensing and GIS. He has received an undergraduate degree in geology, an MS is digital photogrammetry and remote sensing, and an MA in Geomatics. Email: mohammad.ahmed2@ucalgary.ca

Dr. Khan R. Rahaman is a researcher at the Department of Geomatics Engineering and a member of the Earth Observation for Environment Laboratory. His research interests include but not limited to: (i) climate change and local warming trend modeling; (ii) disaster management and resilience; (iii) integrating remote sensing and GIS data to model environmental issues for landuse planning; and (iv) urban sustainability management. He has received an undergraduate in urban and rural planning, an MSc in spatial planning, an MA in environmental studies, and PhD in urban planning. Email: krrahama@ucalgary.ca

Appendix: Case Study of the 2011 Slave Lake Wildland-induced Fire

The Town of Slave Lake is considered as another case study area, which is a mid-sized municipality strategically located in the north central Alberta. This municipality area is situated at a distance of approximately 260 km northwest from the nearest metropolitan city of Edmonton. The population of Slave Lake is approximately 6,651 [19], which has not been growing much in last 30 years. The climate of Slave Lake area is considered as severe during winters, and mild to warm and dry summers for only three months. The daily average temperature in January and July for the Slave Lake area during 1981-2010 were recorded -14.5 and +15.6 ^{o}C, respectively [23]. The Slave Lake area falls under the 'Central Mixedwood' natural subregions of Alberta [24], which is surrounded by thick boreal forest.

In this study, we primarily used three key datasets, such as: (i) space-borne QuickBird satellite imagery received from DigitalGlobe Foundation acquired on 18 May 2011, (ii) historical imageries available from Google Earth Pro system, and (iii) statistical ground data of the damaged structures from NFID. In case of the QuickBird imagery, it had both panchromatic spectral band operating between 0.45 and 0.9 µm with spatial resolution of 0.6m; and multispectral (MS) bands [i.e., blue (0.45-0.52 µm), green (0.52-0.60 µm), red (0.63-0.69 µm), and near infrared (0.76-0.90 µm)] with a spatial resolution of 2.4m. In case of ground-based estimates of structural damages, we enquired the NFID system using several key attributes that are described in the following Table.

TABLE A-1: DESCRIPTION OF THE ATTRIBUTES USED TO ENQUIRE THE NFID SYSTEM FOR EXTRACTING WILDLAND FIRE-INDUCED STRUCTURAL DAMAGES IN CASE OF 2011 SLAVE LAKE FIRE.

Variable Name	Description	Value Used
JURIS	Reporting Jurisdiction	48
YEAR	Year of Incident	2011
MONTH	Month of Incident	5
DATE	Date of Month of Incident	14, 15, 16
INCIDLOC	Incident Location	SLAVE LAKE
IGNIOBJ	Igniting Object	820 Exposure, structure detached 850 Exposure to "open" fire (includes campfire, bonfire, warning flare, rubbish fire, "open" incinerator) 860 Exposure, forest, trees 880 Exposure, vehicle (as described in Section B - property classifications 8400 to 8890) 890 Exposure - unclassified or unknown
IGNOBGRP	Igniting Object Group	8000 Exposure

Since the Slave Lake area is relatively small, we identified the structural damages by visual interpretation from the QuickBird satellite image, and showed in Figure A-1. We found that 378 number of structural damages occurred at the community-level derived from satellite image. We then compared these counts with the ground-based estimates derived from the incident data of

NFID system; and found strong relations (i.e., 378 from satellite image vs. 407 from NFID system). The rationales of such discrepancies were, in fact, described in sub-section "structural damage assessment" under "Results and Discussion" in this report.

FIGURE A-1: THE SPATIAL EXTENT OF THE STRUCTURAL DAMAGE DERIVED FROM QUICKBIRD MS SATELLITE IMAGE.

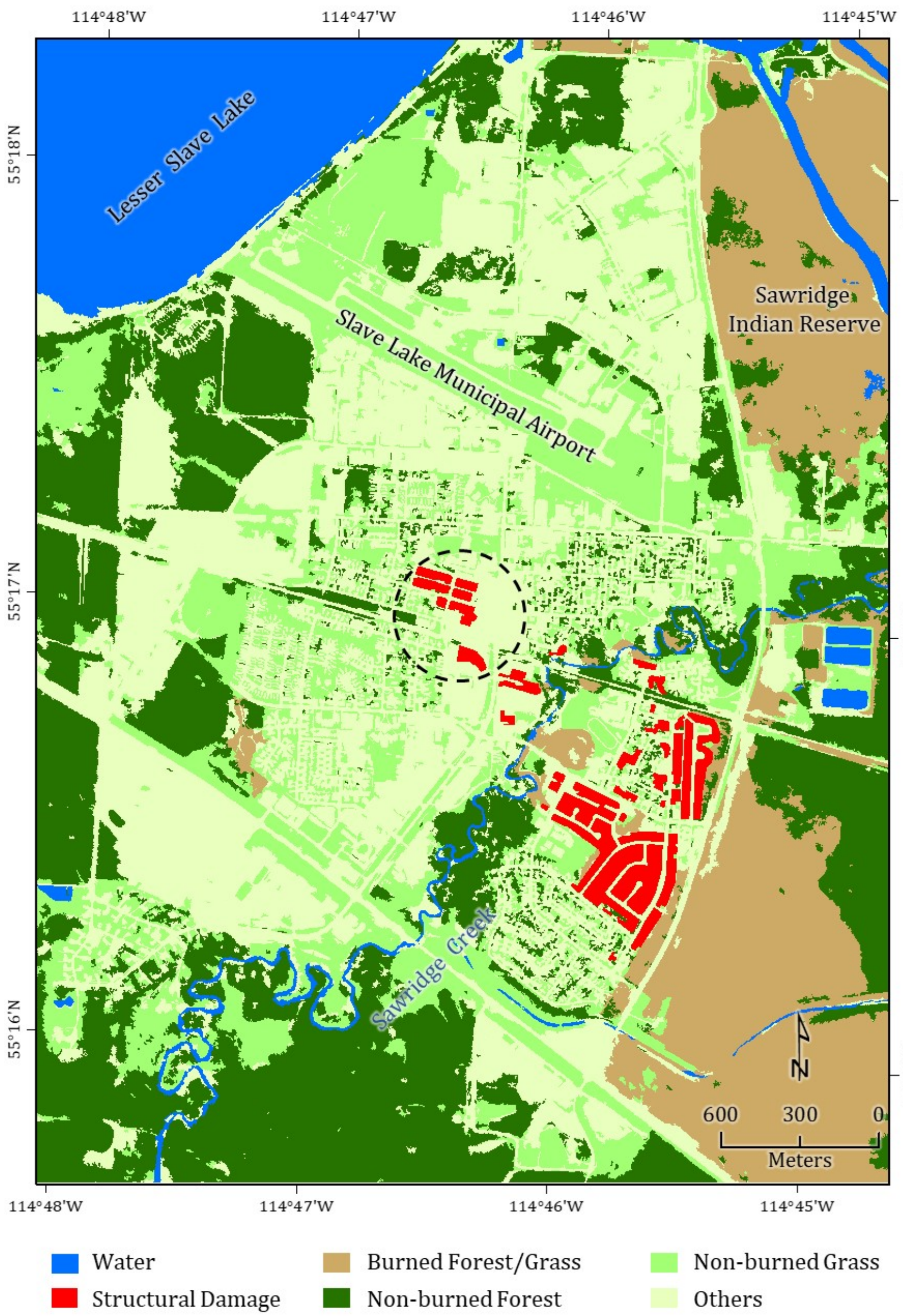

Similar to the 2016 HRF event in Fort McMurray, we also found that there was presence of vegetation within the 10m to 30m buffers from the WUI in most of the instances (see Figure A-2 for example cases) in case of the associated areas with observed structural damages. Note that we also found an exceptional area (see Figure A-1 within the circled zone) of structural damages without having vegetation nearby; which might have happened as the wind might carry ember from the wildland fire from a relatively distant place.

FIGURE A-2: EXAMPLES OF AREAS OF WILDLAND FIRE-INDUCED STRUCTURAL DAMAGES WHERE THERE WAS PRESENCE OF VEGETATION (FUEL FOR FIRE PROPAGATION) WITHIN 10M AND 30M BUFFERS FROM THE WUI.

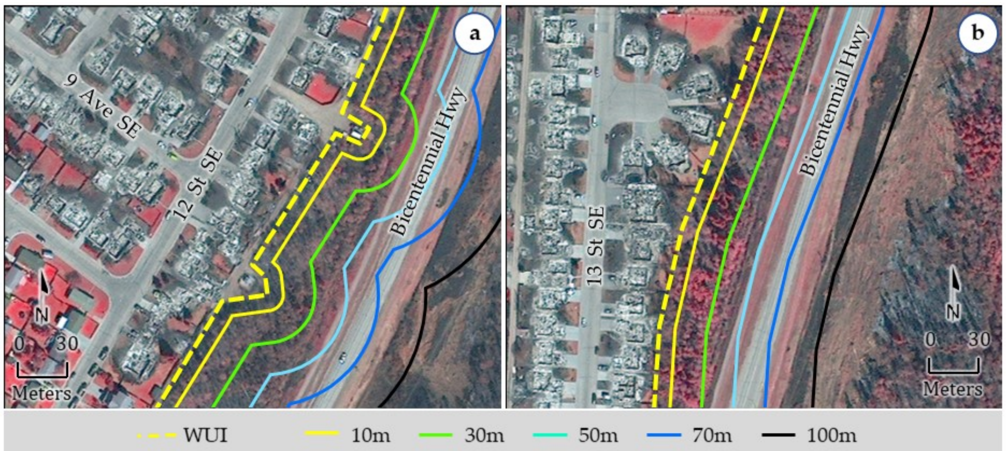

Similar to the Fort McMurray area, we also looked into the wildland fire-induced vulnerable areas upon considering the WUI and its associated buffers. We found that there were still some communities that had the existence of vegetation within the buffer zones (see examples in Figure A-3). In such circumstances, we would recommend that the vegetation should be removed. Also, in order to reduce the wildland fire-induced risks for the communities, it would be critical to have a regular monitoring system in place to assess the vegetation conditions and remove them if deemed necessary as discussed earlier.

FIGURE A-3: EXAMPLES OF WILDLAND FIRE-INDUCED VULNERABLE AREAS.

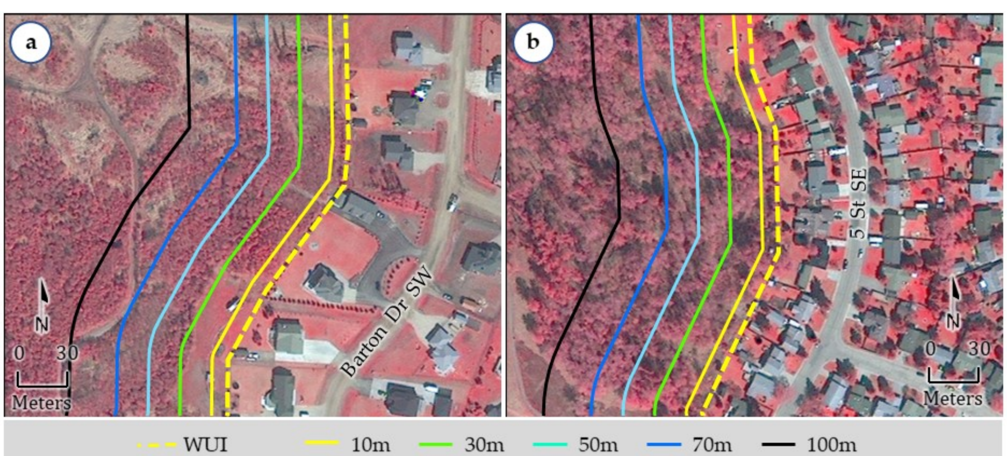

UNIVERSITY OF THE FRASER VALLEY
CENTRE FOR PUBLIC SAFETY & CRIMINAL JUSTICE RESEARCH

SCHULICH
School of Engineering
UNIVERSITY OF CALGARY